RSC Advances

PAPER

View Article Online
View Journal | View Issue

Cite this: *RSC Adv.*, 2025, **15**, 31620

Role of hydrothermally prepared CeO_2 in developing chitosan-based functional coating for banana preservation

Thuong Thi Nguyen, *[ac] Bao-Tran Tran Pham, [bc] Dinh Thien Le,[de] Bang-Tam Thi Dao[de] and Chi Nhan Ha Thuc*[de]

This work aims to construct a nanocomposite coating made from chitosan (CS) and hydrothermally prepared ceria nanoparticles ($hCeO_2$ NPs), and thoroughly evaluate its influence on extending the lifespan of post-harvest bananas over a 12-day period. The $hCeO_2$ NPs were characterized to confirm their synthesis before being integrated within the CS matrix. The morphological, structural, mechanical, water-, and UV-barrier properties of nanocomposite coating films were determined. Furthermore, the physicochemical properties of the fresh banana, such as visual attributes, peel color, respiration rate, firmness, weight loss, total soluble solids, titratable acidity, ripening rate, and pH, are thoroughly considered throughout storage. Results showed that the water permeability, solubility, swelling index, fracture resistance, and flexibility are significantly enhanced by adding 1–2% (w/w) $hCeO_2$ NPs. Notably, a 3.5- and 1.6-fold increase in the fracture strength and plasticity of CS was achieved by adding 1.5% (w/w) $hCeO_2$ NPs. The great UV-barrier function of the $hCeO_2$-loaded CS nanocomposite coating films in UVB and UVC is found. For banana preservation, the CS-1.5%-$hCeO_2$ nanocomposite coating manifested its superior efficiency in retarding the banana ripening compared to CS, commercial chitosan products, and uncoated fruit, extending the expiration date of fresh bananas without deteriorating the fruit's physicochemical characteristics.

Received 16th July 2025
Accepted 23rd August 2025

DOI: 10.1039/d5ra05091j

rsc.li/rsc-advances

Introduction

Cavendish bananas (*Musa acuminata*) are widely cultivated and distributed throughout Vietnam, serving both domestic consumption and export markets. The widespread distribution and export of bananas is due to their nutritional value as a good source of carbohydrates, particularly natural sugars and dietary fiber.[1] Nevertheless, like climacteric fruits, the ripening of bananas continues after being harvested by the production of ethylene gas, making them highly perishable, resulting in their short shelf life. Furthermore, hot and humid storage environments facilitate microbial spoilage development and accelerate the ripening rate, resulting in 25–50% losses,[2] which adversely impact farmers' income. Therefore, it is imperative to develop a preservation technique for maintaining the lifespan of post-harvest bananas.

To avoid post-harvest losses of bananas, the coating technique has been considered to be efficient and feasible in prolonging the expiration date of fresh fruits because these thin film layers on the fruit skin could control water transfer and reduce physiological metabolism.[3] The coating forms on the fruit surface *via* soaking or spraying liquid. In the spraying method, fine droplets of liquid are deposited on the fruit skin through an atomizer.[4] Specific equipment required for the spraying technique is often inaccessible to developing countries. The soaking technique is considered more suitable and efficient for preserving post-harvest fruits due to its facile operation, cost-effectiveness, remarkable effects, non-toxicity, and high scalability. Chitosan-based coatings have been widely and commercially utilized to prolong the storability of fruits and vegetables such as bananas,[5] apples,[6] tomatoes,[6] and mangoes.[7] Given that chitosan (CS), a linear polysaccharide obtained from crustacean and fungal shells, possesses outstanding innocuous, biocompatible, biodegradable, antibacterial, and film-forming features.[7] Notwithstanding, the utilization of CS as a coating to preserve fruits and vegetables is severely restricted because of inadequate mechanical and barrier properties as well as restrained fresh-preservative effects.[8] The earlier work showed that hydrophilic hydroxyl

[a]*Faculty of Applied Science and Technology, Nguyen Tat Thanh University, Ho Chi Minh City, Vietnam. E-mail: nthithuong@ntt.edu.vn; Tel: +84-985-090-912*

[b]*Nguyen Tat Thanh University Center for Hi-Tech Development, Saigon Hi-Tech Park, Ho Chi Minh City, Vietnam*

[c]*Institute of Applied Technology and Sustainable Development, Nguyen Tat Thanh University, Ho Chi Minh City, Vietnam*

[d]*Faculty of Materials Science and Technology, University of Science, Ho Chi Minh City, Vietnam. E-mail: htcnhan@hcmus.edu.vn*

[e]*Vietnam National University, Ho Chi Minh City, Vietnam*

groups in the side chain of CS facilitated water adsorption and swelling, leading to a loose structure, and as a result, mechanical and barrier properties were poor.[9] To revitalize these disadvantages, a plethora of attempts have been made to introduce other substances into CS coatings/films.

Recently, adding nanoparticles (*i.e.*, TiO_2, ZnO, CuO, CeO_2, and MgO) into the chitosan matrix to revitalize the mechanical behaviors, water resistance, and thermal properties of CS-based coating/film materials has been reported.[10–13] The use of CeO_2 NPs to integrate into packaging materials has been increasing as of late because the CeO_2 NPs are reported to be less harmful than TiO_2 and ZnO.[14] Reportedly, the low CeO_2 dosage (<88 ppm) was considered to be safe and non-cytotoxic for humans and extensively applied in biomedical fields.[15] As follows, the CeO_2 NPs, having curated surface chemistry (Ce^{3+}/Ce^{4+} ratio), showed the ability to scavenge reactive oxygen species and thus improved the oxidative stability of vegetable oils. Furthermore, the Pt/plasma-modified CeO_2 (Pt/CeO_2–P) has been shown to efficiently delay the bananas' ripening due to its excellent ethylene scavenging.[16] Previous work also revealed that adding CeO_2 enhanced the fracture strength, antibacterial activity, and water-barrier property of chitosan and cellulose/xanthan films but caused a significant reduction in their elongation at break.[17,18] In contrast, the addition of 0.5–3.0% (w/w) CeO_2 notably declined the tensile strength of the chitosan/poly (vinyl alcohol), which was in contrast with the mobility of the nanocomposite film.[19] In general, few reports show that the integration of CeO_2 into the film matrix can simultaneously improve the fracture strength, flexibility, and barrier function of the resultant material, which meets compliance with regulatory standards to maintain the integrity and quality of packaged food products. The CeO_2 NPs' size and morphology could significantly affect the intercalation of CeO_2 in the polymer matrix. Different synthesis methods result in variations in particle size, shape, surface area, and crystallinity of CeO_2, all of which affect the material's physical and chemical properties. In the literature, CeO_2 was prepared by co-precipitation, hydrothermal and solvothermal, sol–gel, solution combustion, and green methods.[20–24] Based on our findings, hydrothermal is considered a feasible approach to generate high-purity CeO_2 NPs with desired morphology and size at low temperatures.[25] The CeO_2 prepared under hydrothermal conditions consists of a significant amount of Ce^{3+} species, and in preference to exposing {100} planes, which significantly revitalized the O_2 storage capacity of the network. Briefly, an appropriate technique to generate CeO_2 with a small size to easily intercalate into polymer chains is needed to simultaneously improve the fracture resistance, flexibility, and water function of nanocomposite films.

Given the above context, in this study, CeO_2 NPs prepared under hydrothermal conditions ($hCeO_2$) were incorporated into the CS coating to extend the shelf life of bananas. It is anticipated that the prepared CeO_2 NPs can effectively intercalate and interact with chitosan chains, simultaneously improving the fracture strength, flexibility, and moisture barrier properties of the chitosan-based coating. Few studies have explored using $hCeO_2$ in the CS matrix, with agglomeration issues common in co-precipitation and sol–gel methods.[17,19] However, the use of a CS-$hCeO_2$ coating to prolong the shelf life of postharvest fruits and vegetables has yet to be thoroughly reported. This work is the first to systematically optimize $hCeO_2$ concentration (1–2% w/w) within chitosan matrices, demonstrating a nearly fourfold increase in fracture strength and a twofold increase in flexibility—unlike previous studies that reported trade-offs—and correlating nanoparticle dispersion with a 12-day extension in banana shelf life. Our findings provide a theoretical foundation for targeted reinforcement of chitosan properties using $hCeO_2$ NPs, expanding applications in food preservation materials and helping to mitigate physicochemical changes in banana preservation.

Results and discussion

Characterization of CeO_2

SEM images revealed that hydrothermally prepared CeO_2 exhibits a nano-level structure (Fig. 1A). Notably, the $hCeO_2$ NPs were homogeneous and distinct. As seen in the TEM image, the particles were cubic in shape, and their size was calculated to be around 10–70 nm (Fig. 1B). The Zeta potential of the $hCeO_2$ NPs is – 14.6 ± 4.69 mV (SI Fig. B1), suggesting moderate electrostatic repulsion, which may be insufficient to prevent agglomeration.[26] Thus, slight agglomeration could occur in the as-prepared nanoparticles. XRD analysis was performed on the $hCeO_2$ powder sample to affirm the synthesized $hCeO_2$ structure. As seen in Fig. 1C, the XRD patterns of $hCeO_2$ revealed typical peaks at 28.53°, 33.07°, 47.33°, 55.93°, 58.76°, and 69.07° corresponded to the (111), (200), (220), (311), (222), and (400) planes and matched well with the cubic CeO_2 (JCPDS No. 34-0394).[27] The sharp and narrow peaks indicated the crystalline nature of CeO_2.[28,29] Furthermore, the lack of additional spare peaks in the diffraction phases confirmed that the as-prepared $hCeO_2$ NPs were clean and pure. In addition, the functional groups of the as-prepared $hCeO_2$ NPs were determined through

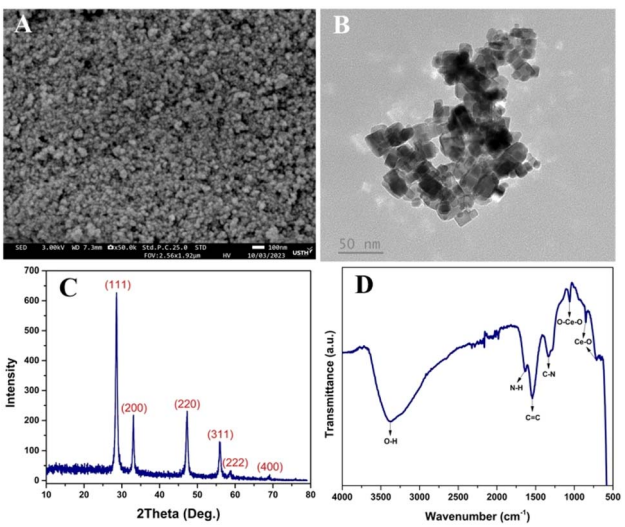

Fig. 1 SEM (A), TEM (B), XRD (C), and ATR-FTIR (D) of CeO_2.

ATR-FTIR analysis (Fig. 1D). The intense band at 3385 cm^{-1} was identified for Ce–OH and remaining alcohols, while the 1632 cm^{-1} was corresponded to the O–C–O stretching and H–O–H flexing, which partially overlapped.[19] The strong absorptive band at 1547 cm^{-1} was indicative of O–H in-plane flexing vibration, and 1328 cm^{-1} referred to the N=O stretching as traces of nitrate.[30] The 1058 cm^{-1} was attributed to the Ce–O–Ce vibration, while those at 848 cm^{-1} and 722 cm^{-1} refer to Ce–O stretching vibration.[31]

Characterization of casting-produced films

Thin film produced from the casting solution is used to evaluate the water resistance and mechanical behaviors of the nanocomposite coatings, which are difficult to completely separate from banana peel surfaces. However, the casting-produced films' properties partly predicted the effectiveness of barrier coating in prolonging the banana's lifespan to some extent due to dissimilar thicknesses. In the current work, the utilization of the same volume of the coating solution on banana preservation to generate CS–$hCeO_2$ films was performed to prevent variations.

Surface morphology

Fig. 2A shows a smooth and relatively uniform surface for the parent CS film. Adding 1–1.5% CeO_2 has minimal influence on the homogeneity of the nanocomposite films (Fig. 2B and C). However, the textured surface of CS-2%-$hCeO_2$ film became rough, with several dots scattered in the matrix due to noticeable $hCeO_2$ nanoparticle clusters (Fig. 2D). High CeO_2 content added into the chitosan matrix yielded a rougher and more heterogeneous film surface. However, no visible separation or cracks were observed on the nanocomposite that significantly impacted the physical properties of the nanocomposite films to some extent. Comparably, the nanocomposite film's surface in this work is smoother and more homogeneous than those found earlier in chitosan[17,32] and chitosan/polyvinyl alcohol[19] integrated with $hCeO_2$. Furthermore, the EDX mapping was implemented to affirm the presence of $hCeO_2$ in the film matrix, as seen in Fig. 2E. A large amount of C and O, along with a small amount of N, were depicted in the EDX spectrum. Apart from C, O, and N, the obvious signal and peak of Ce were also pictured, pointing out the presence of $hCeO_2$ nanoparticles in the CS film.

Visual appearance and light transmission

Visual appearance, color, and see-through functions of packaging films/coatings are vital factors influencing consumers' buying of inside products. The film-forming solution exhibited a slight increase in yellow intensity with increasing $hCeO_2$ content, exhibiting a dose-dependent effect (Fig. 3A). Films prepared from film-forming solutions are flat, shiny, and transparent, as seen in Fig. 3B. The films enriched with $hCeO_2$ became more yellow than the parent CS film. Adding 1–1.5% $hCeO_2$ insignificantly affected the transparency of the nanocomposite films, while the CS-2%-$hCeO_2$ film presented a slightly opaque yellowish color. These outcomes align with the measured color parameters in Table 1 as the *b* value representing yellowness gradually rises. The *L* and WI values of CS-2%-$hCeO_2$ were notably different in comparison with CS-1%-$hCeO_2$ and CS-1.5%-$hCeO_2$ films, indicating the important disparity in lightness and whiteness index of CS-2%-$hCeO_2$ with other film formulas. The see-through and UV-barrier properties of films were appraised by measuring their UV-vis light transmittance (Fig. 3B). The parent CS film presented around 90% light transmittance in the 400–700 nm wavelength range. The light transmittance in these regions of nanocomposite films was an insignificant difference compared to the neat chitosan,

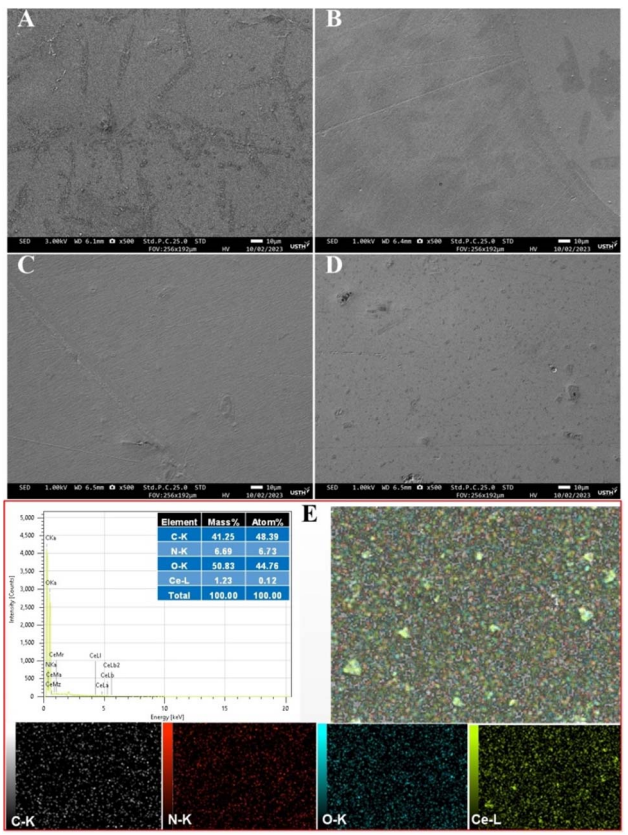

Fig. 2 SEM image of CS (A), CS-1%-$hCeO_2$ (B), CS-1.5%-$hCeO_2$ (C), CS-2%-$hCeO_2$ (D), and EDX mapping of CS-1.5%-$hCeO_2$ film (E).

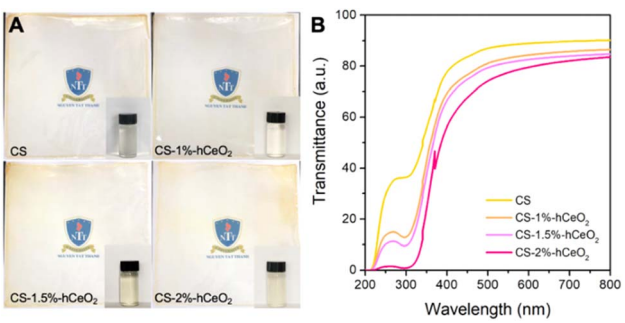

Fig. 3 Coating solution and visual attributes (A) and light transmittance in UV-vis regions (B) of coating solution-produced films.

Table 1 Color parameters of films[a]

Film formulation	L	a	b	WI	ΔE
CS	$91.61^{a} \pm 0.10$	$3.41^{b} \pm 0.03$	$5.20^{a} \pm 0.05$	—	—
CS-1%-$hCeO_2$	$91.08^{a} \pm 0.15$	$3.57^{a} \pm 0.05$	$5.42^{b} \pm 0.07$	$88.97^{a} \pm 0.13$	$0.61^{a} \pm 0.14$
CS-1.5%-$hCeO_2$	$91.16^{a} \pm 0.69$	$3.58^{a} \pm 0.06$	$6.21^{c} \pm 0.07$	$88.61^{a} \pm 0.54$	$1.25^{b} \pm 0.19$
CS-2%-$hCeO_2$	$89.90^{b} \pm 0.17$	$3.02^{c} \pm 0.05$	$11.66^{d} \pm 0.10$	$84.28^{b} \pm 0.19$	$6.70^{c} \pm 0.14$

[a] Different letters within each column indicate significant differences among film formulations based on the Tukey HSD test ($p < 0.05$).

confirming their good transparency, as viewed in the color study and visual attributes. In terms of UV light transmittance (200–400 nm), the parent CS film had a very limited UV resistance compared to that of chitosan films embedded with $hCeO_2$. For instance, at 200–320 nm, the light transmittance of CS-1%-$hCeO_2$ and CS-1.5%-$hCeO_2$ films was around 15% lower than the transmittance of neat CS films (40%). Noticeably, the CS-2%-$hCeO_2$ revealed near-zero light transmittance in these wavelength ranges, indicating that UV transmission through the nanocomposite films was considerably weakened in a comparable view with the CS films, likely by the UV-shielding ability of $hCeO_2$ nanoparticles. Our findings aligned with the previous work, where UV resistance for the polystyrene matrix was reported by embedding CeO_2 nanoparticles.[33]

ATR-FTIR and XRD

ATR-FTIR analysis was performed to verify possible intermolecular interactions between chitosan and $hCeO_2$ in the matrices. The spectrum data of neat chitosan and nanocomposite films are displayed in Fig. 4A. The parent CS film presented characteristic bands at 3352 cm^{-1} and 3282 cm^{-1} (O–H and N–H stretching vibrations), 2928 cm^{-1} and 2881 cm^{-1} (C–H stretching vibration), 1640 cm^{-1} (C═O stretching vibration), 1560 cm^{-1} (stretch of N–H), 1416 cm^{-1} (–C–N stretch), 1035 cm^{-1} (C–O vibration).[34] Adding $hCeO_2$ nanoparticles showed no additional peaks in the nanocomposite film spectra, implying the absence of new covalent bonds among nanoparticles and chitosan. However, slight movements in the position of C═O, N–H, and –C–N stretching vibrations were detected. For instance, a subtle shift from 1640 cm^{-1} to 1649 cm^{-1} (C═O vibration) occurred at CS-1%-$hCeO_2$ and CS-1.5%-$hCeO_2$, and to 1653 cm^{-1} and 1646 cm^{-1} for CS-2%-$hCeO_2$. A slight movement in the peak position at 1561 cm^{-1} (N–H vibration) and 1416 cm^{-1} (–C–N vibration) was observed for the CS-2%-$hCeO_2$ film. Furthermore, the peak at 659 cm^{-1} was left-shifted to 661 cm^{-1} for CS-1%-$hCeO_2$ and CS-2%-$hCeO_2$ and to 663 cm^{-1} for CS-1.5%-$hCeO_2$. The shift in the typical peaks of the nanocomposite film spectra was due to the intermolecular and hydrogen bonding interactions between chitosan and $hCeO_2$.[17,32]

The effect of $hCeO_2$ nanoparticles on the structural property of the chitosan matrix was appraised using XRD. As seen in Fig. 4B, the CS film presents a wide peak of $2\theta = 20.02°$, confirming a characteristic semi-crystalline property of CS. With the introduction of CeO_2, the distinctive peaks of the cubic structure of $hCeO_2$ were observed in the CS-2%-$hCeO_2$ film, while the CS-1%-$hCeO_2$ and CS-1.5%-$hCeO_2$ only presented a weak peak of 28.53°. In addition, the XRD patterns of CS-1%-$hCeO_2$ and CS-1.5%-$hCeO_2$ films showed clearer and more defined peaks than the parent CS film. The existence of

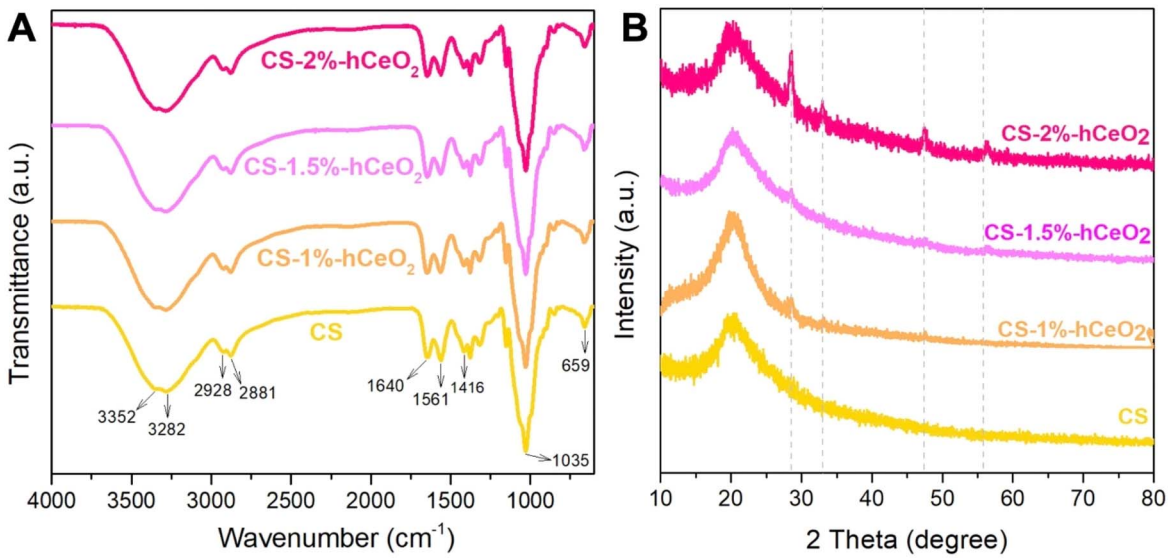

Fig. 4 ATR-FTIR (A) and XRD (B) of films.

characteristic peaks in $hCeO_2$ demonstrated the efficient incorporation of $hCeO_2$ into the CS matrix. In the case of minimal or weak interaction between polymer and nanoparticles, the individual diffraction patterns were distinct and correlated proportionally to the content of each component. Contrarily, the distinctive diffraction patterns of nanofiller components were invisible, likely attributed to strong interactions among components, resulting in significant structural modifications. Herein, the nanoparticles in content below 2% could efficiently interact with the chitosan matrix than 2% $hCeO_2$ added, consistent with enhanced tensile strength and elongation at break in the further investigation.

Mechanical properties

Good mechanical behavior of packaging/coating materials has a competitive edge in resisting external stress during handling, transport, and storage.[35] The film's thickness is first considered due to its significant effect on fracture resistance and the flexibility of packaging materials. Reportedly, a film thickness below 0.3 mm was favored to protect inside food products and prevent oxidative food ingredients.[36] Herein, the film fabrication was performed by spreading the same volume of film-forming solution on plastic molds to avert possible variations. Table 2 reveals an insignificant difference in the thickness of nanocomposite films. The solid ingredient content of film-forming solutions positively affected the film thickness. Adding a small amount of $hCeO_2$ insignificantly increased the solid content of chitosan film (see SI Table B1), resulting in relatively slight thickness modifications. In this work, the mechanical behavior of films was assessed through tensile strength (T_s) and elongation at break (E_{ab}) measurement, as seen in Table 2. The ANOVA analysis exhibited a significant difference in T_s and E_{ab} parameters among (i) the chitosan films loaded and unloaded $hCeO_2$ nanoparticles and (ii) nanocomposite films with varying $hCeO_2$ content. The incorporation of $hCeO_2$ noticeably enhanced the T_s of the parent CS film. For instance, the CS-1%-$hCeO_2$ and CS-1.5%-$hCeO_2$ films revealed a 3- and 3.5-fold increase in the T_s value compared to the neat CS material. This pattern underscores the crucial role of $hCeO_2$ as a great reinforcement to enhance fracture resistance under external force. These significant enhancements could result from hydrogen bonding between chitosan hydroxyl and amine groups with $hCeO_2$, as seen in the ATR-FTIR analyses. However, the higher content of $hCeO_2$ (2% w/w) caused a crucial decrease in the Ts of the resultant film due to the aggregation of CeO_2 in the chitosan matrix. The CS-2%-$hCeO_2$ revealed a nearly 2-fold decrease in the Ts compared to CS-1.5%-$hCeO_2$ and CS-1%-$hCeO_2$. The SEM images also showed CeO_2 nanoparticle clusters on the surface of CS-2%-$hCeO_2$ films, while they were well embedded and dispersed in CS-1%-$hCeO_2$ and CS-1.5%-$hCeO_2$ films. The earlier work reported that the agglomerated nanoparticles facilitate nanocomposite material rupture under external force because the stress is highly concentrated around the aggregates.[12] In addition, a similar trend of T_s was also observed in the E_{ab} of nanocomposite films under the reasons mentioned earlier. The CS-1.5%-$hCeO_2$ had the highest E_{ab} value, where E_{ab} was enhanced 1.6-fold compared to the pure chitosan film. Interestingly, our finding revealed that the same small amount of $hCeO_2$ loaded into chitosan could three- and two-fold improve the T_s and E_{ab} of the nanocomposite films, much more efficiently than what was previously reported, where T_s only increased by 15–28%, and E_{ab} was significantly reduced.[17] What's more, the 5% (w/w) CeO_2 addition caused a significant reduction in the E_{ab} and an insignificant modification in the T_s of chitosan film.[32] Furthermore, adding 1.5% (w/w) CeO_2 also provoked a significant decrease in the T_s of the polyvinyl alcohol/chitosan films.[19] The size of the CeO_2 NPs and their interaction with the chitosan matrix were held accountable for the improvement in the T_s and E_{ab}. The difference in CeO_2 size could come from the different preparation procedures. Herein, CeO_2 prepared *via* the hydrothermal method has a much smaller size below 70 nm than the reported CeO_2 size[17,32] and thereby could well-intercalate into the polymer chains and efficiently interact with chitosan, resulting in enhanced T_s and E_{ab}. Overall, in a comparable view to the previous report, incorporating a small amount of $hCeO_2$ into the chitosan matrix in the current work reaps important benefits from notably improving the fracture strength and flexibility, as great merit for packaging materials.

Water resistance

The water barrier functions of packaging/coating materials are important to prevent physiological water losses of post-harvested fruits and prolong their life span. The water vapor permeability (WVP) of the parent CS film was 11.96×10^{-11} g m m^{-2} Pa^{-2} s^{-2} (Table 3). The earlier works reported that adding nanoparticles resulted in reduced WVP values of chitosan film because tortuous paths were produced.[35,37,38] Similarly, the introduction of $hCeO_2$ significantly improved the water-barrier properties of nanocomposite films, as evidenced by a statistical decrease in the WVP of CS-1.5%-$hCeO_2$ (11.05×10^{-11} g m m^{-2} Pa^{-2} s^{-2}) and CS-2%-$hCeO_2$ (10.77×10^{-11} g m m^{-2} Pa^{-2}

Table 2 Thickness and mechanical properties (tensile strength and elongation at break) of films[a]

Film formulation	Thickness (mm)	Tensile strength (MPa)	Elongation at break (%)
CS	$0.05^{a} \pm 0.00$	$2.80^{a} \pm 0.18$	$44.59^{a} \pm 2.06$
CS-1%-$hCeO_2$	$0.05^{a} \pm 0.00$	$8.71^{c} \pm 0.62$	$65.85^{bc} \pm 1.83$
CS-1.5%-$hCeO_2$	$0.06^{b} \pm 0.00$	$9.92^{c} \pm 0.27$	$71.67^{c} \pm 3.26$
CS-2%-$hCeO_2$	$0.055^{ab} \pm 0.01$	$5.86^{b} \pm 0.51$	$62.47^{b} \pm 1.57$

[a] Different letters within each column indicate significant differences among film formulations based on the Tukey HSD test ($p < 0.05$).

Table 3 Moisture content, solubility, swelling index, and water vapor permeability of films[a]

Film formulation	WVP ($\times 10^{-11}$ g m m^{-2} Pa^{-2} s^{-2})	Solubility (%)	Swelling index (%)
CS	11.96^{a} ± 0.05	24.28^{a} ± 0.21	114.90^{a} ± 1.84
CS-1%-hCeO$_2$	11.65^{a} ± 0.42	22.11^{b} ± 0.80	110.36^{b} ± 1.65
CS-1.5%-hCeO$_2$	11.05^{b} ± 0.11	21.17^{b} ± 1.18	108.69^{b} ± 4.06
CS-2%-hCeO$_2$	10.77^{b} ± 0.39	19.63^{c} ± 0.24	101.32^{c} ± 0.62

[a] Different letters within each column indicate significant differences among film formulations based on the Tukey HSD test ($p < 0.05$).

s^{-2}). Observably, the increase in hCeO$_2$ concentration led to a gradual decrease in the WVP of nanocomposite films. The CeO$_2$ nanoparticles could fill the gaps and defects in the film network and restrict defects, reducing the affinity between the film matrix and water molecules, and thereby decreasing the WVP of films. In other words, the intermolecular interaction between CS and hCeO$_2$ could block hydrophilic groups, which struggle to transmit the water vapor through substrates. Briefly, the hCeO$_2$-loaded-CS nanocomposite films possessed a good water-barrier function, which gave them an advantage in food packaging.

Low water solubility (WS) is favored for food packaging materials to avoid dissolving and losing functionality when exposed to a humid food environment. As seen in Table 3, the CS film presented a WS of 21.43%, which is equivalent to the earlier work.[11] Adding 1–2% (w/w) hCeO$_2$ positively impacted the water resistance when the WS of nanocomposite films gradually decreased from 22.11% to 19.63%. This decrease in WS could be due to the formation of hydrogen bonding between CS and hCeO$_2$, which revitalized the adhesion between polymer chains and restricted the diffusion of water molecules into the film matrices.[19] Similarly, the swelling degree of nanocomposite films also decreased compared to the CS film (Table 3), as explained by the aforementioned reasons. Overall, the reduced water solubility and swelling degree of chitosan films by doping hCeO$_2$ was a great signal to keep the structural integrity of packaging materials under various humid conditions.

Properties of barrier coating films on banana peel surface

The protective nanocomposite coating on the banana surface, formed by dipping, can be washed off with water before eating. Based on the obtained results, the CS-1.5%-hCeO$_2$ nanocomposite coating presents the best fracture resistance, flexibility, and water-barrier ability. Thus, it is chosen as the research object to evaluate the fresh-preservation performance of the nanocomposite coatings on post-harvest bananas. Fig. 5 illustrates the micro-level surface of uncoated and coated fruit. The stomatal structure was seen in all banana groups, according to the earlier reports.[39,40] CS and CS-1.5%-hCeO$_2$ coatings were evenly decorated on the pericarp surface with completely sealed stomata, compared to uncoated fruit, in which some fractures and cleavage between epidermal cells appeared. Kadozan coating exhibited a rougher surface, suggesting its insufficient spreading ability on banana peels. The CS-1.5%-hCeO$_2$-coated fruit revealed a smoother surface than the CS- and Kadozan-coated fruit. Additionally, the size and shape of the stomatal aperture of the fruit coated with CS-1.5%-hCeO$_2$ were modified, likely by good adhesion and/or interaction between the CS–CeO$_2$ coating and epidermal cells of banana peels. Briefly, the surface morphology indicated good dispersion and uniform decoration of CS-1.5%-hCeO$_2$ nanocomposite coating on the banana peel, further reducing the bananas' respiration rate and moisture loss throughout storage.

Evaluation of the effectiveness of barrier coating

Visual appearance is often utilized as a crucial criterion to evaluate the quality and marketability of bananas. The fruit peel color alters from green to yellow during the ripening process by the breakdown and degradation of the green pigment chlorophyll and the generation of new pigments, namely carotenoids.[41] As seen in Fig. 6, the non-coated fruit fully turned yellow on day 4, while Kadozan- and CS-coated fruit were on day 6, except for those treated with CS-1.5%-hCeO$_2$ coating. By day 6, the development of black pigment on the epidermis was observed for the control group before they were spoiled on the 8th day. The enzymatic browning in banana peels comes from the oxidation of phenolic compounds to generate quinones in the epidermis before polymerizing into brown pigments.[42] The brown pigments slowly developed on fruit skin treated with Kadozan and CS on day 8, which were then spoiled on day 10.

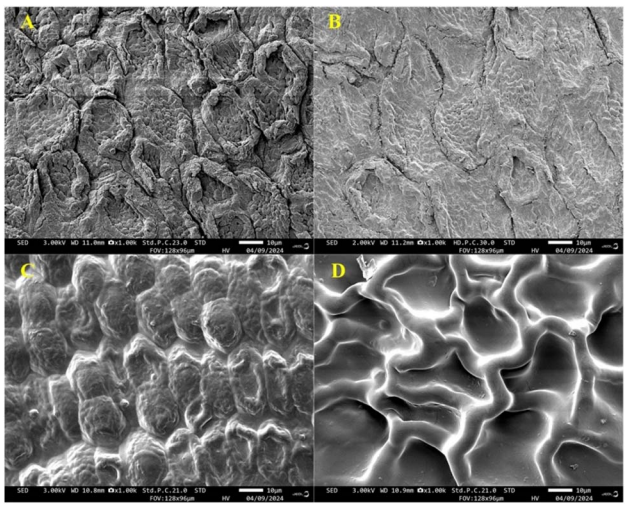

Fig. 5 SEM images of the peel surface of banana without coating (A) and coated with Kadozan (B), CS (C), and CS-1.5%-hCeO$_2$ (D).

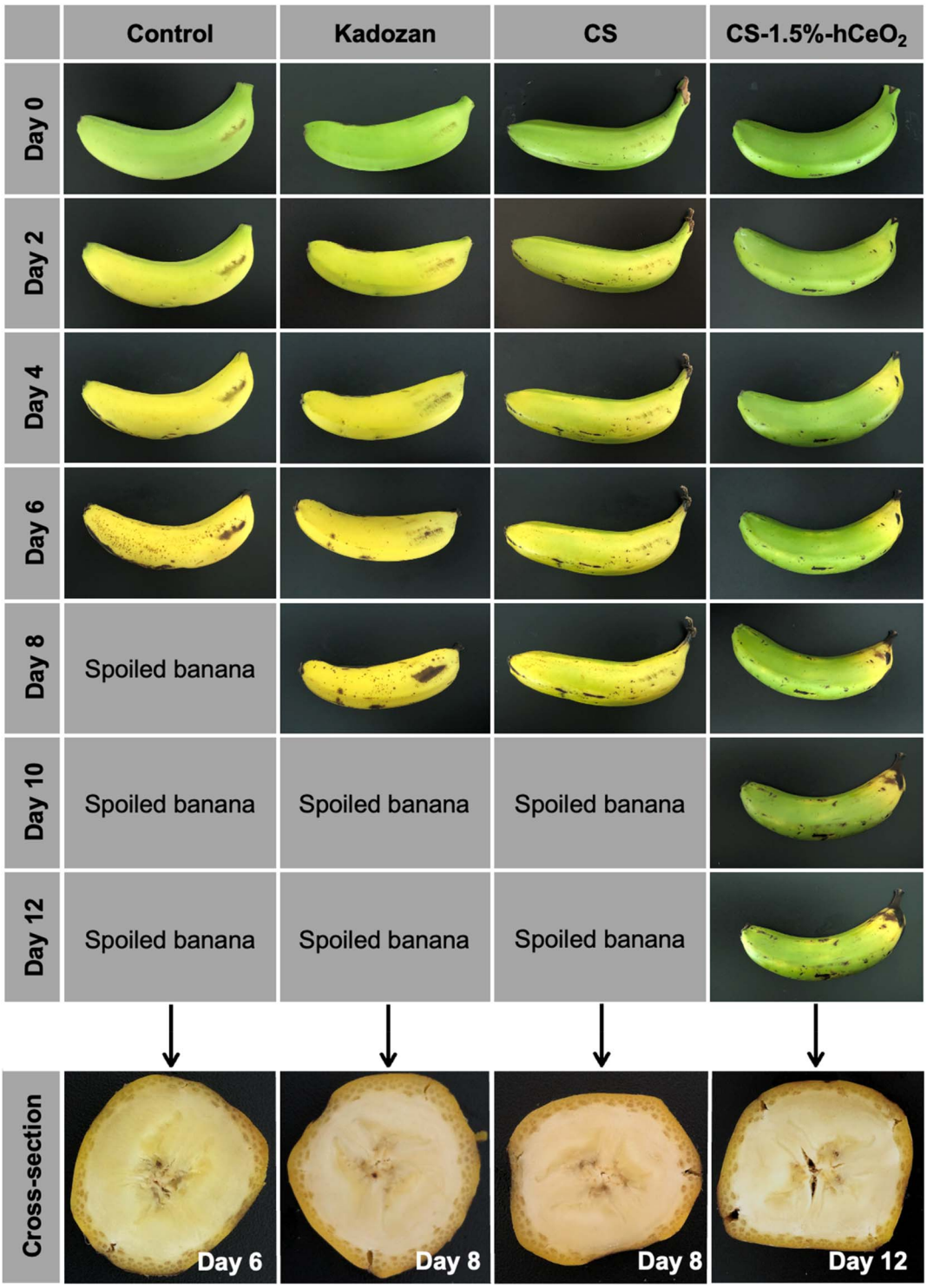

Fig. 6 Visual images of uncoated and coated bananas during 12 d of storage at 20 °C.

The ripening process of CS-1.5%-$hCeO_2$-coated fruit behaved differently when the peel color only turned fully yellow after the storage period. By adding CeO_2 into the chitosan matrix, the fresh-preserving performance of the banana was significantly revitalized, evidenced by the partially yellow appearance of the banana peel after 12 days of storage. This outcome likely resulted from the slow degradation rate of chlorophyll by retarding the respiration rate and moisture losses from bananas. The change in peel color is also confirmed by the color parameters (L, a, and b) of bananas, which indicate the fruit's lightness, greenness, and yellowness during ripening (Table 4). Similar to visual appearance, the L, a, and b parameters

Table 4 Color changes of the banana during storage[ab]

Coating × day	*L*	*a*	*b*
Control × day 0	$56.72^{ab} \pm 1.17$	$-18.32^{ab} \pm 0.2$	$36.80^{ab} \pm 1.7$
Kadozan × day 0	$56.06^{a} \pm 2.26$	$-18.5^{a} \pm 1.72$	$36.7^{ab} \pm 0.27$
CS × day 0	$55.35^{a} \pm 1.93$	$-17.87^{ab} \pm 0.62$	$34.80^{a} \pm 1.71$
CS-1.5%-$hCeO_2$ × day 0	$55.76^{ab} \pm 4.0$	$-17.11^{abc} \pm 0.63$	$35.31^{a} \pm 2.24$
Control × day 2	$66.77^{efghi} \pm 1.71$	$-10.47^{ef} \pm 0.33$	$48.79^{cdef} \pm 2.71$
Kadozan × day 2	$66.15^{defghi} \pm 1.19$	$-9.53^{fg} \pm 0.32$	$51.36^{efgh} \pm 2.63$
CS × day 2	$59.78^{abcd} \pm 1.26$	$-15.89^{c} \pm 0.82$	$36.78^{ab} \pm 1.17$
CS-1.5%-$hCeO_2$ × day 2	$55.88^{a} \pm 4.06$	$-16.53^{bc} \pm 1.03$	$38.82^{ab} \pm 1.96$
Control × day 4	$71.36^{hi} \pm 0.68$	$-3.27^{h} \pm 0.42$	$51.81^{fgh} \pm 3.27$
Kadozan × day 4	$69.05^{ghi} \pm 2.95$	$-3.19^{h} \pm 0.69$	$57.06^{i} \pm 0.8$
CS × day 4	$63.17^{bcdefg} \pm 5.66$	$-13.98^{d} \pm 3.52$	$46.89^{cd} \pm 0.63$
CS-1.5%-$hCeO_2$ × day 4	$60.97^{abcde} \pm 15.06$	$-9.47^{fg} \pm 2.24$	$45.7^{c} \pm 2.96$
Control × day 6	$68.03^{fghi} \pm 0.58$	$-0.69^{ij} \pm 0.79$	$50.98^{efgh} \pm 1.26$
Kadozan × day 6	$72.18^{i} \pm 0.51$	$-1.07^{ij} \pm 0.16$	$53.96^{hi} \pm 5.82$
CS × day 6	$67.62^{fghi} \pm 2.77$	$-12.15^{de} \pm 0.19$	$40.11^{b} \pm 5.51$
CS-1.5%-$hCeO_2$ × day 6	$69.3^{ghi} \pm 1.47$	$-8.12^{g} \pm 0.05$	$47.93^{cdef} \pm 0.9$
Control × day 8	—	—	—
Kadozan × day 8	$61.79^{abcdef} \pm 1.58$	$0.34^{k} \pm 0.59$	$52.94^{gh} \pm 2.0$
CS × day 8	$58.09^{abc} \pm 0.86$	$-11.63^{e} \pm 0.51$	$37.40^{ab} \pm 1.22$
CS-1.5%-$hCeO_2$ × day 8	$71.28^{hi} \pm 1.63$	$-4.09^{h} \pm 0.71$	$49.91^{defg} \pm 0.61$
Control × day 10	—	—	—
Kadozan × day 10	—	—	—
CS × day 10	—	—	—
CS-1.5%-$hCeO_2$ × day 10	$65.16^{defgh} \pm 0.84$	$-2.51^{hi} \pm 0.83$	$47.51^{cde} \pm 0.62$
Control × day 12	—	—	—
Kadozan × day 12	—	—	—
CS × day 12	—	—	—
CS-1.5%-$hCeO_2$ × day 12	$64.36^{cdefg} \pm 0.27$	$-0.21^{k} \pm 0.58$	$45.98^{cd} \pm 1.29$

[a] (–): spoiled fruit. [b] Different letters within each column indicate significant differences among coating formulations at different storage periods using the Tukey HSD test ($p < 0.05$).

gradually increased, suggesting a color change from green to yellow before the appearance of the black spots. The *L* and *b* values of the control group rapidly rose and reached a peak on day 4, and then gradually decreased in the further days of storage, confirming their complete ripening on the 4th day and subsequent development of a brown degree. The fruit treated with CS-1.5%-$hCeO_2$ revealed a slower increment in the *L*, *a*, and *b* parameters than other fruit groups. The obtained results indicated that a CS-1.5%-$hCeO_2$ coating could significantly revitalize the peel color and postpone banana ripening, aligning with Fig. 6.

Bananas, like other climacteric fruits, revealed a significant increase in respiration rate during ripening due to metabolic changes. Thus, the bananas' respiration should be regulated to prolong their expiration date. In general, the coated fruit had a lower amount of CO_2 produced than the uncoated fruit (Fig. 7A). The respiration rate of non-coated fruit reached the climacteric peak with 338.74 mg CO_2 kg^{-1} h^{-1} on day 4 of storage, while Kadozan and CS coated fruit revealed a lag of climacteric peak on the sixth day with 285.62 mg CO_2 kg^{-1} h^{-1} and 284.66 mg CO_2 kg^{-1} h^{-1}, respectively. Interestingly, the CS-1.5%-$hCeO_2$ coating delayed the climacteric peak of the banana on day 8 with 267.51 mg CO_2 kg^{-1} h^{-1}. The lowest and slowest respiration rate of fruit treated with CS-1.5%-$hCeO_2$ compared to other groups manifested its efficiency in slowing the fruit's respiration rate. As reported, chitosan-based coatings have been shown to reduce respiration activity, resulting in slower ripening and extended shelf life of bananas.[43] The coating could offer an optional permeability, which slowed down the O_2 flow and enabled CO_2 permeation in fruit. The addition of $hCeO_2$ might lengthen the path of O_2 through the chitosan matrix and restrain the respiration rate of the banana. Of particular interest is the observation that the CS-1.5%-$hCeO_2$ treatment could reduce the amount of CO_2 produced and regulate the respiration process of bananas.

Mass loss of all groups increased with the advancement of the storage time (Fig. 7B), explained by the water and carbohydrate losses through transpiration and respiration activities during storage.[44] Generally, the fruit without and with Kadozan and CS coatings had an equivalent weight loss of 13.50%, 12.83%, and 12.11%, respectively, after 6 days of storage, two-fold higher than those of CS-1.5%-$hCeO_2$-coated fruit (7.29%). It was supported by the fact that CS-1.5%-$hCeO_2$ coating film demonstrated the more superior water-barrier function in comparison with CS as discussed above. The 13.51% weight loss of CS-1.5%-$hCeO_2$-coated fruit on day 10 was equivalent to that on day 6 of the banana without coating. In general, it is of utmost importance to highlight that the CS-1.5%-$hCeO_2$ presented the lowest percentage of weight loss during storage compared to other treatments, considering the significant economic benefits of using CS-1.5%-$hCeO_2$ coating in banana preservation.

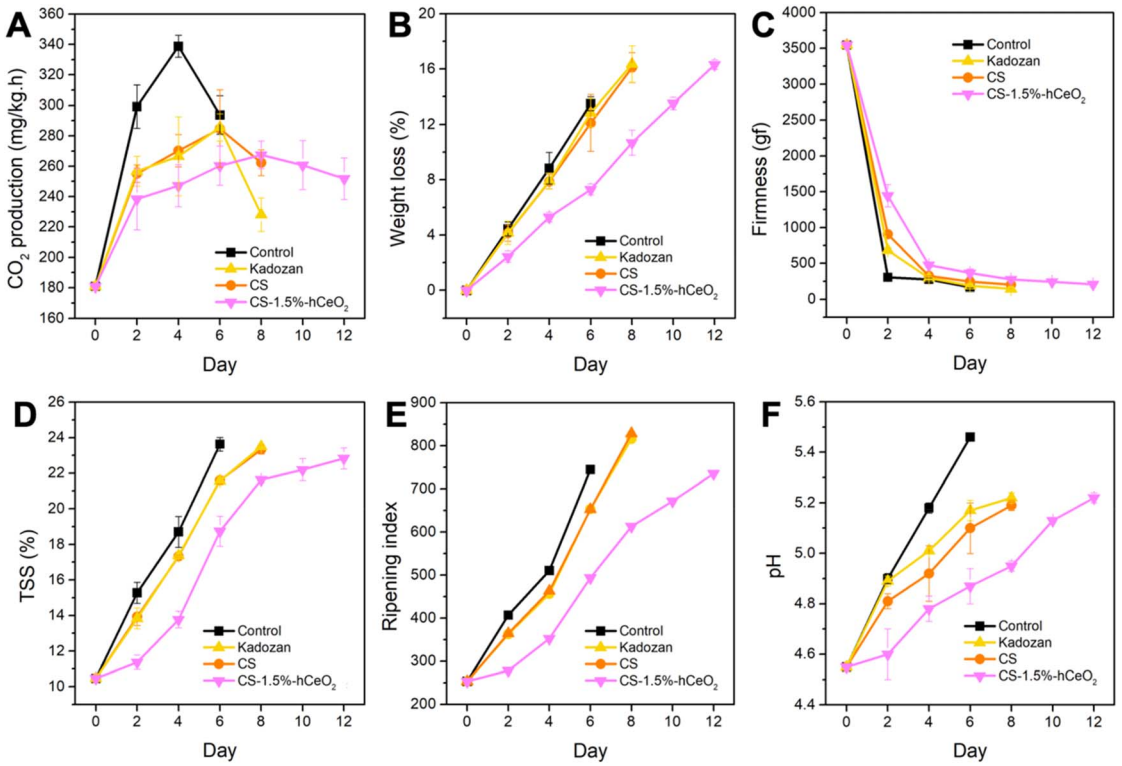

Fig. 7 Changes in CO_2 production (A), weight loss (B), firmness (C), total soluble solids content (D), titratable acidity (E), and pH (F) of bananas during storage.

Fruit firmness is directly associated with banana ripeness, which affects to buying decision of customers and therefore it is considered a crucial indicator of banana quality aspects. Fig. 7C reveals a downward trend in the fruit firmness throughout storage, mainly due to metabolic activities arising from the complex respiration occurring in pectic, cell wall polysaccharides, and starch.[45] The CS-1.5%-$hCeO_2$ coating was a more significant barrier to fruit softening compared to other coatings, when a slower decrease in firmness was recorded. For instance, the data from the sixth-day measurement showed that 365.91 gf firmness of CS-1.5%-$hCeO_2$ was twofold higher than the control and Kadozan groups. The 275.60 gf measurement of CS-1.5%-$hCeO_2$-coated fruit was equivalent to the firmness at day 4 of the uncoated fruit, suggesting that CS-1.5%-$hCeO_2$ coating can reduce the softness of bananas throughout storage.

The total soluble solids content (TSS) is a crucial banana parameter when reflecting the fruit's taste and ripening. As seen in Fig. 7D and SI Table B2, the TSS of all groups tends to increase as a function of storage time. The increment in TSS was closely related to sugar levels (sucrose, glucose, and fructose) produced from starch and carbohydrate metabolism.[46] The non-coated fruit exhibited a more rapid increment in TSS in comparison to the coated groups. For instance, the TSS values of control, Kadozan, CS, and CS-1.5%-$hCeO_2$ on day 6 of storage were 23.63%, 21.57%, 21.60%, and 18.73%, respectively. The generation from the conversion of carbohydrate compounds that occurred in the fruit ripening process was closely related to the fruit's respiration rate. A slower increase in the TSS of coated fruit might result from a lower internal O_2 level due to barrier coating on the banana peel. The CS-1.5%-$hCeO_2$-coated fruit exhibited the slowest changes in TSS value during storage, suggesting that this coating formulation could retard the conversion of carbohydrate compounds in bananas. The ripening index also has a similar trend with the TSS, as seen in Fig. 7E, indicating the fresh-preservative performance of CS-1.5%-$hCeO_2$ coating in delaying fruit ripening. Similarly, Mwakalesi and Umbayda[47] reported that the chitosan enriched with ZnO slowed the increase in the TSS and ripening index of fruit during the entire storage. The increment in the pH of fruit aligned with those in TSS and the ripening index. The reduction in malic and citric acids likely holds partial responsibility for the increase in the pH parameter. As observed, the pH of the control group linearly increased with the storage time. The fruit treated with CS-1.5%-$hCeO_2$ had the slowest increment in the pH compared to CS- and Kadozan-coated fruit. Briefly, a slower surge in TSS, ripening index, and pH of CS-1.5%-$hCeO_2$-coated fruit than other groups, highlighted that this coating formulation possibly delays the conversion to sugars from starch and carbohydrates during storage, and thus, it could extend the shelf life of post-harvest banana.

Experimental

Chemicals and materials

Chitosan (M_w: 190 000–310 000 Da and DD: 75–85%) was provided by Sigma-Aldrich (USA). Cerium(III) nitrate

hexahydrate [$Ce(NO_3)_3 \cdot 6H_2O$] was purchased from Shanghai Zhanyun Chemical Co., Ltd (China). Other chemicals were acquired from Xilong Scientific Co., Ltd (China).

Preparation and characterization of CeO_2 nanoparticles

The CeO_2 nanoparticles used in this assay were prepared using a hydrothermal-based technique, as described by Wen Lou *et al.*[48] Firstly, dissolving 1.92 g of $Ce(NO_3)_3 \cdot 6H_2O$ into 40 mL of water was performed under magnetic stirring for 30 min. Subsequently, 20 mL of 2 M NaOH was added to the as-prepared solution to obtain a white precipitate. Next, the resulting solution was poured into the Teflon–lined stainless steel autoclave before being dried at 180 °C for 24 h and then left to cool at room temperature (27 °C). The yellow precipitate was centrifuged and washed using ethanol (96%) and distilled water until reaching pH = 7. Finally, the as-prepared sample was dried overnight at 80 °C to remove moisture before being calcined in a muffle furnace at 400 °C for 2 h (5 °C min^{-1}) to obtain the finished product. The CeO_2 preparation was confirmed using X-ray diffraction (XRD), zeta potential, scanning electron microscope (SEM), attenuated total reflectance Fourier-transform infrared (ATR-FTIR), and transmission electron microscopy (TEM), as described thoroughly in Section A.1 of the SI.

Film fabrication and characterization

Chitosan and chitosan-CeO_2 films were fabricated by the solvent evaporation method. Briefly, dissolving 1 g of chitosan into 100 mL of 1% (v/v) acetic acid was carried out by magnetically stirring for 24 h to have a 1% (w/v) chitosan solution. A plasticized chitosan solution was prepared by adding 30% (w/w based on the weight of chitosan) glycerol into the as-prepared chitosan solution and vigorously stirring for 60 min. The above-prepared CeO_2 nanoparticles (1–2% w/w based on the weight of chitosan) were added into the plasticized chitosan solution, and nanocomposite solutions were magnetically stirred until CeO_2 was well-dispersed in the polymer matrix. The as-fabricated homogeneous solutions were poured into the 200 × 200 mm polypropylene molds before being further dried at 50 °C in the Memmert oven for 72 h to obtain the nanocomposite films. The chitosan films doped with different amounts of 0%, 1%, 1.5%, and 2% of CeO_2 nanoparticles were marked as CS, CS-1%-hCeO_2, CS-1.5%-hCeO_2, and CS-2%-hCeO_2, respectively. All nanocomposite films were conditioned at 27 °C in desiccators for 24 h before being further characterized. All coating films were characterized by SEM, energy dispersive X-ray (EDX), ATR-FTIR, XRD, thickness, and mechanical behavior. The water vapor permeability, water solubility, and swelling index of all films were also investigated. The color, visual attributes, and light transmittance of films were recorded. The detailed information was well-described in Section A.2 of the SI.

Application of coating solution for banana preservation. In this work, the soaking technique was selected for further improvement in spreadability and adhesion, along with its convenience, such as facile operation, time- and labor-saving.[49] Briefly, 270 Cavendish bananas (*Musa acuminata*) were sourced from the agricultural market in Ho Chi Minh City with uniform maturity (yellowish green), size, and weight. To eliminate impurities, these fruits were washed under running water and then dried using forced airflow at room temperature (27 °C). After that, they were randomly divided into the control (uncoated) group, Kadozan (coated) group, CS (coated) group, and CS-1.5%-hCeO_2 (coated) group. Next, the fruit were individually dipped in the as-prepared coating solution for 4 s and then dried for 30 min. Each batch was replicated three times due to the preliminary assays to achieve the desired coating thickness on the fruit surface. Uncoated and coated fruit were stored at 20 °C and 64% RH for 12 d. Sensory and physicochemical changes in fruit during storage were appraised every 2 d. In this context, fruit coated with Kadozan (commercial chitosan formula, Lytone Enterprise, China) contained 2% (w/v) food-grade chitosan with the deacetylation of >95% and the molecular weight is 20–30 kDa,[50,51] as a positive control. The coating surface, respiration rate, mass loss, pulp firmness, total soluble solids content, titratable acidity, pH, and ripening rate were characterized with the detailed information provided in Section A.3 of the SI.

Statistical analyses

Statistical significance was determined through ANOVA analyses using STATGRAPHICS Centurion XV software. Significant differences among mean values were obtained at $p < 0.05$ using the Tukey HSD test.

Conclusions

This study reported on a nanocomposite coating formulated by CS and hCeO_2 NPs with enhanced mechanical strength and water- and UV-barrier functions effectively for post-harvest banana preservation. The introduction of hCeO_2 NPs enhanced the fracture strength and flexibility of the nanocomposite films by 3.5- and 1.6-fold, respectively. An enhancement in water and UV resistance of the nanocomposite materials by adding hCeO_2 NPs was achieved. Preservation experiments of fresh bananas revealed that CS-1.5%-hCeO_2 nanocomposite coating could delay the respiration rate, mass loss, softening, ripening, total soluble solid, and pH of bananas and prolong their shelf life by 12 days, which was more efficient than fruit coated with chitosan and a commercial product (Kadozan). The outstanding outcome in the current work has industrial potential for extending the shelf life and the freshness of perishable fruits. However, the delay in the banana ripening related to the reduction in the ethylene production on fruit coated with CS-1.5%-hCeO_2 coatings, as well as intermolecular interaction between CS and hCeO_2 NPs, is still not fully understood in the current work, which will be further investigated to develop these coatings for commercial application.

Author contributions

Thuong Thi Nguyen: writing–original draft, conceptualization, writing–review & editing. Bao-Tran Tran Pham: methodology, investigation, formal analysis, data curation. Dinh Thien Le:

methodology, formal analysis. Bang Tam Thi Dao: formal analysis, data curation. Chi Nhan Ha Thuc: conceptualization, supervision, project administration, writing–review & editing.

Conflicts of interest

There are no conflicts to declare.

Data availability

Supplementary information: The data supporting this article have been included as part of the SI. See DOI: **https://doi.org/10.1039/d5ra05091j**.

Acknowledgements

This research is funded by Vietnam National University, Ho Chi Minh City (VNU-HCM) under grant number 562-2025-18-03. We acknowledge Nguyen Tat Thanh University, Ho Chi Minh City, Vietnam, for supporting the analytical equipment in this study.

References

1 B. Singh, J. P. Singh, A. Kaur and N. Singh, *Food Chem.*, 2016, **206**, 1–11.
2 W. Ma, Y. Zhang, L. Chen, X. Xie, S. Yuan, Z. Qiu, G. Zhu and J. Guo, *Int. J. Biol. Macromol.*, 2024, **281**, 136559.
3 S. Sasidharan, L.-H. Tey, S. Djearamane, N. K. M. Ab Rashid, R. PA, V. Rajendran, A. Syed, L. S. Wong, V. K. Santhanakrishnan, V. S. Asirvadam and A. C. T. Antony Dhanapal, *Food Packag. Shelf Life*, 2024, **43**, 101298.
4 J. Jiang, P. S. M. S. L. Watowita, R. Chen, Y. Shi, J.-T. Geng, K. Takahashi, L. Li and K. Osako, *Food Packag. Shelf Life*, 2022, **32**, 100842.
5 T. T. Nguyen, B.-T. T. Pham, D. V. Nguyen, L. G. Bach and C. N. Ha Thuc, *Sci. Hortic.*, 2024, **328**, 112942.
6 L. Jiang, F. Wang, X. Xie, C. Xie, A. Li, N. Xia, X. Gong and H. Zhang, *Int. J. Biol. Macromol.*, 2022, **209**, 1307–1318.
7 T. Wang, Z. Yang, C. Zhang, X. Zhai, X. Zhang, X. Huang, Z. Li, X. Zhang, X. Zou and J. Shi, *Int. J. Biol. Macromol.*, 2022, **222**, 2843–2854.
8 W. Zhang and J.-W. Rhim, *Food Packag. Shelf Life*, 2022, **31**, 100806.
9 T. Yan, C. Hu, Y. Que, Y. Song, D. Lu, J. Gu, Y. Ren and J. He, *Int. J. Biol. Macromol.*, 2023, **253**, 126668.
10 U. Siripatrawan and P. Kaewklin, *Food Hydrocolloids*, 2018, **84**, 125–134.
11 X. Sun, H. Wang, H. Liang, N. Meng and N. Zhou, *Food Hydrocolloids*, 2025, **159**, 110686.
12 R. T. De Silva, M. M. M. G. P. G. Mantilaka, S. P. Ratnayake, G. A. J. Amaratunga and K. M. Nalin de Silva, *Carbohydr. Polym.*, 2017, **157**, 739–747.
13 M. N. Gunaki, S. P. Masti, O. J. D'souza, M. P. Eelager, L. K. Kurabetta, R. B. Chougale, A. J. Kadapure and S. K. Praveen Kumar, *Food Hydrocolloids*, 2024, **152**, 109937.
14 M. Appu, H. Wu, H. Chen and J. Huang, *Environ. Sci. Pollut. Res.*, 2022, **30**, 42575–42586.
15 S. Chakraborty, K. R. Sahoo, D. Bera, C. K. Ghosh and L. Roy, *Food Chem.*, 2025, **472**, 142834.
16 H. Wei, L. Li, T. Zhang, F. Seidi, Q. Chen and H. Xiao, *ACS Appl. Nano Mater.*, 2023, **6**, 3738–3749.
17 S. D. Purohit, R. Priyadarshi, R. Bhaskar and S. S. Han, *Food Hydrocolloids*, 2023, **143**, 108910.
18 M. Mesgari, M. M. Matin, E. K. Goharshadi and M. Mashreghi, *Int. J. Biol. Macromol.*, 2024, **273**, 133091.
19 M. H. Ali, S. K. Dutta, M. S. Sultana, A. Habib and P. K. Dhar, *Int. J. Biol. Macromol.*, 2024, **280**, 135976.
20 B. S. Wee, S. A. bin E. Halim and T. F. Choo, *J. Cluster Sci.*, 2024, **35**, 2061–2068.
21 Y. Xu, Y. Zhou, Y. Li, Y. Liu and Z. Ding, *J. Environ. Chem. Eng.*, 2024, **12**, 113719.
22 H. Nosrati, M. Heydari and M. Khodaei, *Mater. Today Bio*, 2023, **23**, 100823.
23 L. D. Sonawane, A. S. Mandawade, L. N. Bhoye, H. I. Ahemad, S. S. Tayade, Y. B. Aher, A. B. Gite, L. K. Nikam, S. D. Shinde, G. H. Jain, G. E. Patil and M. S. Shinde, *Inorg. Chem. Commun.*, 2024, **164**, 112313.
24 M. Ramachandran, R. Subadevi and M. Sivakumar, *Vacuum*, 2019, **161**, 220–224.
25 T. Divya, C. Anjali, K. R. Sunajadevi, K. Anas and N. K. Renuka, *J. Solid State Chem.*, 2021, **300**, 122253.
26 S. A. ul. H. Gillani, M. U. Zahid, Z. Ali, M. Zafar, M. A. Khan, N. T. B. Talha, S. M. Almutairi, H. A. Haseeb and S. A. I. Bokhari, *Plasmonics*, 2025.
27 A. Xie, W. Liu, S. Wang, X. Liu, J. Zhang and Y. Yang, *Mater. Res. Bull.*, 2014, **59**, 18–24.
28 G. Ren, L. Wang and S. Wang, *Colloids Surf., A*, 2025, **705**, 135764.
29 X. Zhuang, E. Magnone, S. W. Han and J. H. Park, *Ceram. Int.*, 2024, **50**, 24801–24814.
30 R. C. Deus, M. Cilense, C. R. Foschini, M. A. Ramirez, E. Longo and A. Z. Simões, *J. Alloys Compd.*, 2013, **550**, 245–251.
31 A. Arumugam, C. Karthikeyan, A. S. Haja Hameed, K. Gopinath, S. Gowri and V. Karthika, *Mater. Sci. Eng. C*, 2015, **49**, 408–415.
32 V. A. Petrova, N. V. Dubashynskaya, I. V. Gofman, A. S. Golovkin, A. I. Mishanin, A. D. Aquino, D. V. Mukhametdinova, A. L. Nikolaeva, E. M. Ivan'kova, A. E. Baranchikov, A. V. Yakimansky, V. K. Ivanov and Y. A. Skorik, *Int. J. Biol. Macromol.*, 2023, **229**, 329–343.
33 K.-Q. Liu, C.-X. Kuang, M.-Q. Zhong, Y.-Q. Shi and F. Chen, *Opt. Mater.*, 2013, **35**, 2710–2715.
34 C. Qiu, B. Chen, W. Yin, D. J. McClements, Z. Jin and H. Ji, *Food Hydrocolloids*, 2025, **161**, 110881.
35 X. Chang, Y. Hou, Q. Liu, Z. Hu, Q. Xie, Y. Shan, G. Li and S. Ding, *Food Hydrocolloids*, 2021, **119**, 106846.
36 A. M. Ribeiro, B. N. Estevinho and F. Rocha, *Food Bioprocess Technol.*, 2021, **14**, 209–231.
37 T. Yan, Y. Ren, R. Zhang, K. Li, B. Yang, M. Tong and J. He, *Int. J. Biol. Macromol.*, 2025, **295**, 139595.

38 M. I. Hidayat, A. Hardiansyah, K. Khoiriah, E. Yulianti, R. A. K. Wardhani, F. Fahrialdi and M. R. I. Yusuf, *Food Chem.*, 2025, **477**, 143480.
39 Z. Deng, J. Jung, J. Simonsen and Y. Zhao, *Food Chem.*, 2017, **232**, 359–368.
40 A. Wantat, K. Seraypheap and P. Rojsitthisak, *Food Chem.*, 2022, **374**, 131731.
41 P. THOMAS and M. T. JANAVE, *Int. J. Food Sci. Technol.*, 1992, **27**, 57–63.
42 J. Xie, R. Wang, Y. Li, Z. Ni, W. Situ, S. Ye and X. Song, *Food Chem.*, 2022, **375**, 131708.
43 F. M. Dwivany, T. Fauziah, K. Yamamoto, C. Novianti, K. P. Cadu Perwira, M. Rizanti, S. K. Radjasa, F. S. Hakim, A. S. P. Salim, R. R. Putri, A. Wicaksono, D. Sumardi, S. P. Putri, E. Fukusaki, K. Meitha and H. Nugrahapraja, *Hortic., Environ. Biotechnol.*, 2025, **66**, 123–136.
44 G. Luo, J. Li, X. Qin, Q. Wang and J. Zhong, *Food Chem.*, 2024, **460**, 140764.
45 J. Geng, J. O'Dell, N. Stark, P. Kitin, X. Zhang and J. Y. Zhu, *Food Hydrocolloids*, 2024, **150**, 109671.
46 T. Prabha and N. Bhagyalakshmi, *Phytochemistry*, 1998, **48**, 915–919.
47 A. J. Mwakalesi and T. G. Umbayda, *Appl. Food Res.*, 2024, **4**, 100536.
48 W. Luo, J. Rong, W. Zhao, K. Kang, L. Long and X. Yao, *Chem. Eng. J.*, 2022, **444**, 136488.
49 T. Wang, X. Zhai, X. Huang, Z. Li, X. Zhang, X. Zou and J. Shi, *Food Packag. Shelf Life*, 2023, **39**, 101133.
50 Y. Lin, G. Chen, H. Lin, M. Lin, H. Wang and Y. Lin, *Int. J. Biol. Macromol.*, 2020, **165**, 601–608.
51 X. Jiang, H. Lin, J. Shi, S. Neethirajan, Y. Lin, Y. Chen, H. Wang and Y. Lin, *Food Chem.*, 2018, **252**, 134–141.